PERFORMANCE ASSESSMENT OF PTSC-DRIVEN ORGANIC RANKINE CYCLE SYSTEMS INTEGRATED WITH BOTTOMING KALINA AND ABSORPTION CHILLER CYCLES: A PARAMETRIC STUDY

by

Masood DEHGHAN [1], Ghasem AKBARI [*, 1], Nader MONTAZERIN [2], Arman MAROUFI [1]

[1] Department of Mechanical Engineering, Qazvin Branch, Islamic Azad University, Qazvin, Iran

[2] Department of Mechanical Engineering, Amirkabir University of Technology, Tehran, Iran

It is crucial to evaluate the impact of key parameters of multi-generation systems on their performance characteristics in order to develop efficient systems. The present study conducts parametric analysis of a PTSC-driven trigeneration system with a novel energy distribution based on direct-fed organic Rankine cycle (ORC) and bottom-cycled arrangement of double-effect absorption refrigeration cycle and Kalina cycle system. Three different ORC structures (simple, regenerative, and ORC integrated with IHE) are proposed. Effect of key ORC parameters namely ORC evaporator pinch point temperature and pump inlet temperature is examined on the thermodynamic performance of systems. Decrease of pinch point temperature enhances overall efficiencies and heating power in all three configurations, and increases (decreases) the net electrical power for ORC and RORC (ORC) based systems. This also enhances the cooling power of the RORC based system, though it has no impact on the cooling power of the ORC and ORC-IHE based systems. Reduction of the ORC pump inlet temperature increases overall exergy efficiency in all hybrid systems and overall energy efficiency in the ORC and ORC-IHE based systems, whereas it slightly decreases for the RORC based system. Based on a comparative study, performance of the proposed systems is found to be higher than related solar-driven multi-generation systems in the literature.

Key words*: Parabolic trough solar collector; Organic Rankine cycle; Multi-generation; Kalina cycle system; Absorption refrigeration cycle*

1. Introduction

Combined cooling, heating, and power (CCHP) system is one of the most promising technologies to enhance efficiency of stand-alone cycles, reduce energy consumption, and diminish the harmful impacts on the environment [1, 2]. Incorporating solar energy technologies instead of fossil fuel into the CCHP system is an effective solution to mitigate air pollution and global warming [3]. Parabolic trough solar collector (PTSC) is the commonly-used solar thermal technologies for

* Corresponding author, Email: g.akbari@qiau.ac.ir

power generation. Regarding components of CCHP system, organic Rankine cycle (ORC) and Kalina cycle system (KCS) have significant potential to integrate with the solar-driven power generation; ORC because of its compatibility with low to medium temperature heat sources ($60-350$ ℃)[4, 5], and KCS as a bottoming cycle with appropriate thermal match between the input heat source and the working fluid temperature [6]. Absorption refrigeration cycle (ARC) is also the most usual mode for cooling production in solar-driven hybrid systems[7]. Therefore, the present study aims to conduct a parametric study to evaluate performance of novel solar-driven CCHP systems consisting of ORC, KCS and ARC. Related literature is reviewed to clarify the contribution of the present study.

Bellos and Tzivanidis [8] analyzed a PTSC-driven CCHP system consisting of an ORC and a single effect absorption refrigeration cycle (SEARC) and stated that higher solar beam irradiation and greater heat rejection/evaporating temperature leads to higher energetic performance. Ibrahim and Kayfeci [9] performed thermodynamic analysis of a CCHP system driven by PTSC including ORC and ARC. They showed that rise of ambient temperature reduces exergy efficiency of the system. In another study, Gao et al. [10] examined a seasonal solar-driven CCHP system based on ORC and ARC. It was found that thermal efficiency enhances in spring, autumn and winter when ORC evaporation temperature decreases. Zhao et al. [11] investigated sequential and parallel configurations of a PTSC-driven system including ORC and SEARC. Evaporator temperature ranging from 83.9 ℃ to 197.7 ℃ resulted in a higher solar-to-electrical efficiency ranging from 3.20 % to 11.03 %. In another study, the impact of heat source flow rate on efficiency and output powers was examined for a similar system [12]. The optimal mass flow rate of the heat source was obtained to be in the range of 0.1-0.2 kg/s for the highest performance. Jafary et al. [13] conducted parametric study of two PTSC-driven CCHP systems based on regenerative ORCs and double effect absorption refrigeration cycle (DEARC). It was seen that as the condenser pressure increased, energy/exergy efficiency decreased, without a significant effect on turbine inlet pressure. Barbazza et al. [14] indicated that minimum acceptable temperature differences for evaporator and condenser have the highest impact on the output power of a solar-driven ORC system. Eisavi et al. [15] analyzed CCHP system consisting of PTSC, ORC and DEARC. They found that turbine inlet pressure has little impact on the performance, while increase of ORC evaporator pinch point temperature declined the energy and exergy efficiencies. Chen et al. [16] investigated a similar system for building demands and indicated reduction of energy and exergy efficiencies with rising condensation temperature from 50 ℃ to 70 ℃. Examination of a PTSC-driven tri-generation system consisting of ORC, electric heater/chiller and DEARC revealed that direct normal irradiance has a positive impact on the energy efficiency of ORC and DEARC [17].

Cao et al. [18] considered a PTSC-driven CCHP system with ORC and DEARC components and showed that increase of ORC pump inlet temperature led to decrease of energy and exergy efficiencies. Han et al [19] examined a tri-generation system comprising of a solar full-spectrum subsystem, a double-effect absorption heat pump/chiller and an ORC. The results indicated that thermal allocation ratio is directly (inversely) correlated with annual exergy (energy) efficiency. Parametric study of a PTSC-based system including regenerative ORC, SEARC, desalination unit and thermal energy storage was conducted by Xi et al [20] . They showed that increase of pinch point temperature of regenerative ORC (RORC) evaporator resulted in lower energy and exergy efficiencies.

Regarding integration of KCS with solar-powered CCHP systems, the literature is scarce. Ganesh and Srinivas [21] analyzed a PTSC-driven KCS system and indicated that the highest

efficiencies and specific power were achievable at the lowest amounts of separator and turbine inlet concentration. Gogoi and Hazarika [22] examined four configurations of PTSC-driven trigeneration systems consisting of multiple ORCs, direct-fed triple-effect ARC and KCS. They found a higher performance for the hybrid system comprising one KCS and one ORC. In another study, integration of KCS and DEARC with PTSC system resulted in energy and exergy efficiencies of 13.8 % and 6.55 %, respectively [23]. Tariq et al. [24] investigated a solar-driven tri-generation system based on ORC, direct-fed DEARC and KCS and reported the maximum energetic efficiency of 46.30 %.

Investigation of the configurations of ARC in multi-generation systems have indicated that arrangement of ARC as a bottoming cycle feeding by another cycle like ORC leads to higher energy and exergy efficiencies [11, 25, 26]. The bottoming cycle arrangement is more frequent in the solar-driven systems compared to the direct-feeding ARC configuration[15, 27]. From another perspective, SEARC and DEARC systems can consistently operate with heat source temperature in the range of $80-150\ ℃$ and $100-205\ ℃$, respectively [7, 28-30]. Both of these temperature ranges are more consistent with bottom-cycled ARC compared to direct-fed ARC that involves considerably higher input temperature.

The above discussion emphasizes the importance of suitable positioning of various cycles in a multi-generation system in order to extract the optimal output from those cycles as well as from the overall hybrid system. Additionally, acquiring in-depth knowledge about the effect of characterizing parameters is crucial for improvement of system performance. In this regard, the current study proposes a novel energy distribution based on direct-fed ORC and bottom-cycled arrangement of DEARC and KCS for the PTSC-driven tri-generation system. Parametric study of three new tri-generation systems with three different ORC structures (simple, regenerative, and ORC integrated with internal heat exchanger) is conducted in terms of key ORC parameters, namely ORC evaporator pinch point temperature and pump inlet temperature.

The article is organized as follows. The three proposed systems are described in Section 2. It is followed by thermodynamic modeling of the CCHP system and validation of its components in sections 3 and 4, respectively. Section 5 presents the main results, discusses about the prominent findings, and compares performance results of the current study with those of the literature.

2. System description

The tri-generation systems in the present study employ the PTSC as the prime mover and utilize the ORC, KCS, heating process unit and DEARC to generate electrical, heating and cooling power. Three thermal configurations are proposed in the ORC cycle, namely simple ORC, ORC-IHE and RORC systems. These configurations are derived based on a combination of the best practices reviewed in section 1. The heat absorbed by the heat transfer fluid (HTF) in the solar field is directed towards the ORC and KCS systems. The ORC system supplies thermal energy for the heating process unit and the remaining energy is adequate for the high-pressure generator (HPG) of the DEARC system. The solar system is composed of 40 rows of LS-2 collectors, 13 collectors per row. Therminol VP-1 is utilized as the HTF due to its high thermal capacity, reasonable temperature control [31] and ability to operate at temperatures up to 400 ^{o}C [7]. Mass flow rate of HTF per single row of the solar collectors is set to 0.5 kg/s. For the ORC working fluid, n-octane is chosen for its high critical temperature [32].

2.1. ORC-based cycles

In the ORC based system (Figure 1-a), the organic fluid at the HPG outlet (state 32) is pumped to the evaporator to provide the required energy for power generation in turbine. The required heat for the heating process (HP) process and HPG is provided by the turbine outlet fluid (state 35).

The ORC-IHE based system (Figure 1-b) incorporates an intermediate heat exchanger (IHE). The HPG outlet fluid (state 32) is first pumped to the IHE for preheating and then passes through the evaporator and turbine. The turbine outlet fluid (state 36) delivers heat to the IHE and after discharging the IHE, it supplies the thermal energy for HP and DEARC systems.

The RORC based system (Figure 1-c) includes a feed fluid heater (FFH). The HPG outlet fluid (state 32) is pumped to the FFH to be mixed with the high-pressure vapor exiting from the turbine (state 37). This stream is then pumped toward the evaporator and turbine. The low-pressure vapor at the turbine outlet (state 38) supplies the required heat for the HP and DEARC systems.

2.2. Kalina cycle system

All three CCHP systems presented in Figure 1 utilize the KCS11-type Kalina cycle. In KCS system, the working fluid absorbs heat from the HTF in the evaporator (state 5). It then separates into rich ammonia-water saturated vapor (state 6) for power generation and poor ammonia-water saturated liquid (state 7) for regeneration. The poor ammonia-water liquid is throttled to the condenser pressure (state 10), before mixing with the rich ammonia-water expanded from the turbine (state 8). The fluid leaving the condenser (state 12) is then pumped towards the regenerator for pre-heating and toward the evaporator to complete the cycle.

2.3. DEARC system

All three trigeneration systems employ a series-flow double effect LiBr-H_2O absorption chiller, as depicted in Figure 1. To pre-heat the weak solution leaving the absorber (state 28), it is pumped to the low temperature heat exchanger (LTHE) and high temperature heat exchanger (HTHE) before passing through the HPG (state 31). In the HPG, a portion of water evaporates, generating primary refrigerant vapor (state 15) and medium solution (state 22). The medium solution then enters the low-pressure generator (LPG) after passing through HTHE and the expansion valve EV-4. In the LPG, the primary refrigerant vapor condenses (state 16), producing secondary refrigerant vapor (state 18) and strong solution (state 25). After throttling of the condensed primary refrigerant vapor in valve EV-2, it mixes with the secondary refrigerant vapor in the condenser. The refrigerant then enters the evaporator with a significant temperature drop due to heat rejection in the condenser and throttling in the valve EV-1 (state 20). Finally, the strong solution passes through LTHE and expansion valve EV-3, and mixes with the refrigerant vapor (state 21) in the absorber to produce the weak solution (state 28).

2.4. General methodology and assumptions

The present study aims to evaluate the effect of ORC evaporator pinch point temperature and ORC pump inlet temperature (pump 1 in RORC configuration) on the energy flow between cycles and thermodynamic performance characteristics. The analysis begins by setting the input data for the parameters/states of the systems (as listed in Tables 1 and 2). Next, thermodynamic states data are extracted based on the thermophysical properties of the working fluids. The energy and exergy balance equations are then solved to determine various performance metrics, including electrical,

heating, and cooling powers, as well as energy and exergy efficiencies. Thermodynamic analysis is conducted based on some assumptions, namely steady-state condition, dead state pressure/ temperature of 101.325 kPa/298.15 K, negligible pressure drop and friction in the piping system and heat exchangers, minimal change of kinetic and potential energy/exergy, and negligible chemical exergy for the working fluid in DEARC [33]. The states at the condenser and evaporator outlets are considered as saturated liquid and saturated vapor, respectively, and the mixture temperature at KCS separator inlet is set to 30 ℃,which is lower than the dew point.

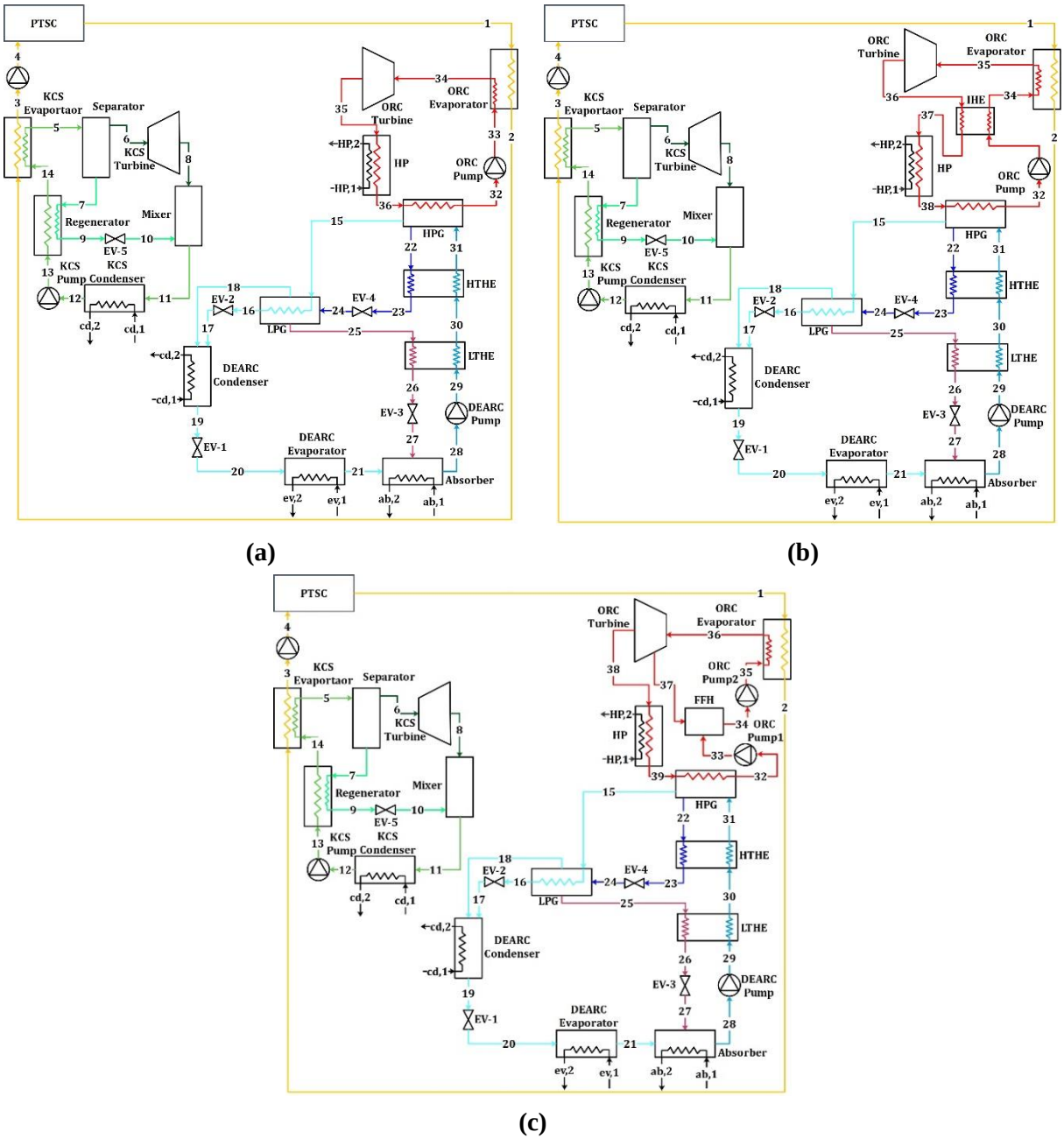

Figure 1. Schematic representation of the ORC based (a), ORC-IHE based (b) and RORC based (c) trigeneration systems.

Table 1. Input data for PTSC [34, 35].

Parameter	Symbol	Value	Parameter	Symbol	Value
Geometrical parameters					
Width	W	5 m	Length	L	7.8 m
Focal length	F	1.71 m	Concentration ratio	C	22.74
Receiver inner area	A_{ri}	1.617 m^2	Receiver outer area	A_{ro}	1.715 m^2
Cover inner area	A_{ci}	2.671 m^2	Cover outer area	A_{co}	2.818 m^2
Receiver inner diameter	D_{ri}	0.066 m	Receiver outer diameter	D_{ro}	0.070 m
Cover inner diameter	D_{ci}	0.109 m	Cover outer diameter	D_{co}	0.115 m
Aperture area	A_{ap}	39 m^2	Number of rows	N_r	40
Optical/operating parameters					
Receiver emittance	ε_r	0.2	Cover emittance	ε_{cov}	0.9
Receiver absorptivity	α	0.96	Cover transmissivity	τ	0.95
Intercept factor	γ	0.99	Concentrator reflectivity	ρ_{con}	0.83
Incident angle	θ	0°	Incident angle modifier	$K(\theta = 0°)$	1
Maximum optical efficiency	$\eta_{opt,max}$	75 %	Solar beam intensity	G_b	800 W/m^2
HTF mass flow rate at each row	$\dot{m}_{HTF}$	0.5 kg/s	HTF temperature at the collector inlet	T_4	55 ℃

Table 2. Input data for ORC (three arrangements), DEARC and KCS.

Cycle/Parameter	Value	Ref.	Cycle/Parameter	Value	Ref.
ORC/KCS			**DEARC**		
Turbine isentropic efficiency	0.9	[22]	HPG temperature	120 ℃	[15]
Pump isentropic efficiency	0.9	[22]	Condenser temperature	35 ℃	[15]
Electrical generator efficiency	0.95	[15]	Absorber temperature	35 ℃	[15]
Electrical motor efficiency	0.95	[15]	Evaporator temperature	7 ℃	[15]
Regenerator effectiveness	0.75	[22]	LPG pinch point temperature	5 ℃	[15]
ORC turbine inlet pressure	2000 kPa	[15]	Effectiveness of solution heat exchangers	0.7	[15]
ORC feed fluid heater pressure	500 kPa	[36]	Solution pump efficiency	0.95	[15]
ORC pump inlet temperature	123 ℃				
KCS condenser temperature	30 ℃	[22]			
KCS separator inlet pressure	35				
NH_3 concentration at KCS separator inlet	0.9	[22]			

A numerical code is developed in MATLAB® to solve the governing equations and post-process the results. It is linked with Engineering Equation Solver (EES®) to extract thermodynamic properties of various working fluids and states. Mathematical modeling of the proposed hybrid systems is described in the following section.

3. Mathematical modeling

3.1. Parabolic trough solar collector

The useful solar heat gain can be obtained as follows [35]:

$$\dot{Q}_u = K_1 \dot{Q}_S - K_2 \left({T_{in}}^4 - {T_{amb}}^4 \right) \quad (1)$$

where the coefficients K_1 and K_2 can be calculated from Table 3. T_{in} and T_{amb} represent the temperature at HTF receiver inlet and ambient temperature, respectively. $\dot{Q}_S$ notifies the solar beam irradiation, defined as:

$$\dot{Q}_S = A_{ap} G_b \quad (2)$$

where G_b and A_{ap} presents solar beam intensity and collector aperture area, respectively. Considering $\dot{Q}_u$ as the thermal input and employing energy balance on the solar collector, the HTF outlet temperature is obtained as follows [35]:

$$T_{out} = T_{in} + \dot{Q}_S \left(\frac{K_1}{\dot{m} c_P} \right) - \left(\frac{K_2}{\dot{m} c_P} \right) \left({T_{in}}^4 - {T_{amb}}^4 \right) \quad (3)$$

where c_P and $\dot{m}$ are constant-pressure specific heat and mass flow rate of HTF, respectively.

3.2. Thermodynamic analysis

Performance of the trigeneration systems is evaluated in terms of energy and exergy metrics, as follows.

3.2.1 Energy analysis metrics

Considering $\dot{W}_{net}^{ORC}$ and $\dot{W}_{net}^{KCS}$ as net electrical power of ORC and KCS cycles, electrical energy efficiency of these cycles is calculated as follows [9]:

Table 3. Definition of coefficients K_1 to K_5 used in the PTSC modelling [34, 35].

Coefficient	Definition	Coefficient	Definition
${K_1}^{*}$	$\eta_{opt} \left[1 + \frac{4 {T_{in}}^3 K_3}{K_4} \right]^{-1}$	${K_4}^{***}$	$\left[\frac{1}{h_{fm} A_{ri}} + \frac{1}{2 \dot{m} c_P} \right]^{-1}$
K_2	$K_3 \left[1 + \frac{4 {T_{in}}^3 K_3}{K_4} \right]^{-1}$	K_5	$A_{co} \varepsilon_{co} \sigma {T_{amb}}^3 + A_{co} h_{co,o}$
${K_3}^{**}$	$A_{ro} \varepsilon_r' \sigma \left[1 + \frac{4 {T_{amb}}^3 A_{ro} \varepsilon_r^* \sigma}{K_5} \right]^{-1}$		

* η_{opt} represents optimal efficiency of the collector, expressed as $\eta_{opt} = K(\theta) \rho_{con} \gamma \tau \alpha$, where $K(\theta)$ is the incident angle modifier coefficient, given as [37]:

$K(\theta) = 1 - 2.2307 \times 10^{-4} \theta - 1.1 \times 10^{-4} \theta^2 + 3.18596 \times 10^{-6} \theta^3 - 4.85509 \times 10^{-8} \theta^4$

** ε_r' is expressed as $\varepsilon_r' = \left[\frac{1}{\varepsilon_r} + \frac{1 - \varepsilon_c}{\varepsilon_c} \left(\frac{A_{ro}}{A_{ci}} \right) \right]^{-1}$

*** h_{fm} represents convective heat transfer coefficient for the internal flow inside the absorber pipe, expressed as $h_{fm} = 0.023 k (Re^{0.8} Pr^{0.4}) / D_{ri}$ [35].

$$\eta_{el,ORC} = \frac{\dot{W}_{net}^{ORC}}{\dot{m}_{ev}^{ORC}\left(h_{ev,out}^{ORC} - h_{ev,in}^{ORC}\right)}, \tag{4}$$

$$\eta_{el,KCS} = \frac{\dot{W}_{net}^{KCS}}{\dot{m}_{ev}^{KCS}\left(h_{ev,out}^{KCS} - h_{ev,in}^{KCS}\right)}, \tag{5}$$

Generally, $\dot{W}_{net}$ for each cycle or multi-generation system is defined as follows [38]:

$$\dot{W}_{net} = \sum \dot{W}_{tur}\eta_g - \sum \frac{\dot{W}_{pump}}{\eta_m}, \tag{6}$$

where η_m and η_g represent efficiencies of pump electromotor and electrical generator, respectively.

COP of the DEARC system is defined as follows [22, 39]:

$$COP_{DEARC} = \frac{\dot{m}_{ev}^{DEARC}\left(h_{ev,out}^{DEARC} - h_{ev,in}^{DEARC}\right)}{\dot{m}_{HPG}^{ORC}\left(h_{HPG,in}^{ORC} - h_{HPG,out}^{ORC}\right) + \dot{W}_{pump}^{DEARC}}, \tag{7}$$

where $\dot{W}_{pump}^{DEARC}$ is pump power consumption, and $\dot{m}_{HPG}^{ORC}$ and $\dot{m}_{ev}^{DEARC}$ denote mass flow rate of the ORC fluid passing through HPG and evaporator mass flow rate in the DEARC system, respectively.

The overall energy efficiency of the system is calculated as follows [15]:

$$\eta_{el,overall} = \frac{\dot{W}_{net,overall}}{\dot{Q}_{in}}, \tag{8}$$

where $\dot{Q}_{in}$ represents the input (solar) energy and $\dot{W}_{net,overall}$ is the net electrical power of the overall system, expressed as follows:

$$\dot{Q}_{in} = \dot{m}_{HTF}\left(h_{HTF,out}^{PTSC} - h_{HTF,in}^{PTSC}\right), \tag{9}$$

$$\dot{W}_{net,overall} = \dot{W}_{net}^{ORC} + \dot{W}_{net}^{KCS}. \tag{10}$$

The energy efficiencies for combined heat and power system (η_{CHP}), combined cooling and power system (η_{CCP}) and combined cooling, heat and power system (η_{CCHP}) are defined as follows [15]:

$$\eta_{CHP} = \frac{\dot{W}_{net,overall} + \dot{Q}_{heating}}{\dot{Q}_{in}} \tag{11}$$

$$\eta_{CCP} = \frac{\dot{W}_{net,overall} + \dot{Q}_{cooling}}{\dot{Q}_{in}}, \tag{12}$$

$$\eta_{CCHP} = \frac{\dot{W}_{net,overall} + \dot{Q}_{heating} + \dot{Q}_{cooling}}{\dot{Q}_{in}}, \tag{13}$$

where $\dot{Q}_{heating}$ is heating power in the HP unit, calculated as follows:

$$\dot{Q}_{heating} = \dot{m}_{HP}\left(h_{HP,out} - h_{HP,in}\right). \tag{14}$$

3.2.2 Exergy analysis metrics

The overall exergetic efficiency of system is defined as follows [38]:

$$\Psi_{el,overall} = \frac{\dot{W}_{net,overall}}{\dot{E}x_{coll}} \tag{15}$$

where $\dot{E}x_{coll}$ is the exergy of solar collectors calculated as [38, 40]:

$$\dot{E}x_{coll} = A_{ap,t}G_b\left(1+\left(\frac{1}{3}\right)\left(\frac{T_0}{T_{sun}}\right)^4-\left(\frac{4}{3}\right)\left(\frac{T_0}{T_{sun}}\right)\right) \quad (16)$$

where T_0 is surrounding temperature and T_{sun} is the sun temperature (6000 K) [38].

The exergetic efficiencies for combined heat and power system (Ψ_{CHP}), combined cooling and power system (Ψ_{CCP}) and combined cooling, heat and power system (Ψ_{CCHP}) are defined as follows [38]:

$$\Psi_{CHP} = \frac{\dot{W}_{net,overall} + \dot{E}x_{heating}}{\dot{E}x_{coll}} \quad (17)$$

$$\Psi_{CCP} = \frac{\dot{W}_{net,overall} + \dot{E}x_{cooling}}{\dot{E}x_{coll}} \quad (18)$$

$$\Psi_{CCHP} = \frac{\dot{W}_{net,overall}+\dot{E}x_{heating} + \dot{E}x_{cooling}}{\dot{E}x_{coll}} \quad (19)$$

where $\dot{E}x_{heating}$ represents the heating power exergy in the HP unit and $\dot{E}x_{cooling}$ notifies exergy of cooling in the DEARC evaporator, expressed as follows [41]:

$$\dot{E}x_{heating} = \dot{m}_{HP}\left(ex_{HP,out} - ex_{HP,in}\right) \quad (20)$$

$$\dot{E}x_{cooling} = \dot{Q}_{cooling}\left(\frac{T_0}{T_{ev}^{DEARC}} - 1\right) \quad (21)$$

where T_{ev}^{DEARC} is the temperature of DEARC evaporator.

4. Validation

Mathematical modeling of different sub-systems is verified based on four different studies, as follows:

1. **PTSC system**: Experimental study by Dudly et al. [42] is utilized to verify the PTSC modeling under similar configuration and operating conditions. Table 4 presents the main input data and compares HTF output temperature and thermal efficiency of collector for the present simulations with those of measurements. The relative errors were found to be less than 0.12 % and 2.55 % for output temperature and thermal efficiency, respectively.
2. **ORC-based systems**: The accuracy of thermodynamic models for ORC, ORC-IHE, and RORC cycles is examined by comparing their performance results with the study of Safarian and Aramoun [43]. The relative errors for thermal efficiency are less than 1.8 %, as presented in Table 5.
3. **KCS System**: Considering the same operating condition, numerical results of KCS in the present study are validated with the study of He et al. [44]. Relative errors of the present study in terms of thermal efficiency are found to be less than 1.8 %, as listed in Table 6.
4. **DEARC system**: A DEARC integrated with a CCHP system [15] is utilized for validation of DEARC modeling. Based on identical input heat from the ORC to the DEARC and similar operating conditions, the COP calculated by the present modeling is 1.18, which is exactly identical to the value reported in [15].

Table 4. Comparison of PTSC system results with experimental data of Dudly et al. [42].

	Input data				Results & errors					
	G_b $(\frac{w}{m^2})$	T_{amb} (K)	T_{in} (K)	$\dot{V}$ $(\frac{L}{min})$	T_{out}(K)			η_{en}(%)		
					Present study	Ref. value	Relative error (%)	Present study	Ref. value	Relative Error (%)
1	933.7	294.35	375.35	47.7	397.6	397.15	0.11	73.13	72.51	0.85
2	968.2	295.55	424.15	47.8	447	446.45	0.12	72.25	70.9	1.90
3	982.3	297.45	470.65	49.1	493.1	492.65	0.09	71.18	70.17	1.43
4	909.5	299.35	523.85	54.7	542.5	542.55	0.009	69.4	70.25	1.21
5	937.9	301.95	570.95	55.5	590	590.05	0.008	67.54	67.98	0.64
6	880.6	300.65	572.15	55.6	589.9	590.35	0.07	67.16	68.92	2.55
7	903.2	304.25	629.05	56.3	647.3	647.15	0.02	64.11	63.82	0.45
8	920.9	302.65	652.65	56.8	671.3	671.15	0.02	62.62	62.34	0.44

Table 5. Comparison of the results of three ORC-based cycles with the results reported by Safarian and Aramoun [43].

Cycle	η_{el} (%)		
	Present study	Ref. value	Relative error (%)
ORC	19.63	19.46	0.8
ORC-IHE	21.7	21.5	0.9
RORC	22.4	22	1.8

Table 6. Comparison of KCS cycle results with data reported by He et al. [44].

Input data		Results & errors		
$P_1(MPa)$	X_1	η_{el} (%)		
		Present study	Ref. value	Relative error (%)
1.5	0.59	8.02	7.97	0.6
2	0.69	8.62	8.46	1.8
2.5	0.81	9.34	9.19	1.6
3	0.92	10.28	10.23	0.4

5. Results and discussion

This section investigates the effect of key parameters of the ORC-based cycles on the system performance. Also, a comparison between the present results and literature is performed. Based on the physical and operating data of the PTSC system presented in Table 1 and the methodology described in section 3.1, the HTF temperature at the solar field outlet is calculated to be 339.75 ℃. This temperature is identical for all three tri-generation systems (state 1) which provides the same energy and exergy resource. The input data for modeling of ORCs, KCS and DEARC are summarized in Table 2.

5.1. Parametric study

The effect of two key parameters of the ORC cycles, namely the ORC evaporator pinch point temperature (T_{PP}) and the ORC pump inlet temperature (T_{32}), is examined on the performance of the proposed trigeneration systems. T_{PP} is selected as a key variable because it specifies the minimum

possible temperature difference between the HTF and Organic working fluid (OWF) streams in the ORC evaporator which effectively characterizes the heat balance between ORC and KCS cycles. Furthermore, ORC pump inlet temperature plays an important role because it determines the lower temperature of the ORC cycle and therefore quantifies its Carnot efficiency.

5.1.1 ORC evaporator pinch point temperature

A lower pinch point temperature in the evaporator typically enhances the thermodynamic performance of ORC, though it requires a more extended heat transfer surface area and increases the design cost. The impact of T_{PP} on the system power outputs and energy/exergy efficiency is investigated by considering various temperatures in the range of $12 - 26$ ℃, based on the fixed ORC pump inlet temperature and turbine inlet pressure (123 ℃ and 2 MPa, respectively).

Figure 2 presents the effect of ORC evaporator pinch point temperature on the power outputs of the trigeneration systems in terms of electrical, heating and cooling aspects. For all configurations, increase of T_{PP} decreases the heat transferred to ORC which in turn enhances the thermal heat towards the KCS system. This reduces the OWF outlet temperature, decreases the temperature difference between the inlet and outlet of OWF, and consequently declines the heat transfer from HTF to OWF in the ORC evaporator. Consequently, the OWF leaves the evaporator by a lower enthalpy that in turn declines the turbine power as well as the net electrical power of the ORC cycle for all hybrid systems. On the other side, increase of T_{PP} enhances the thermal input energy of the KCS evaporator and increases the net power output of KCS cycle. Regarding overall electrical power output, the

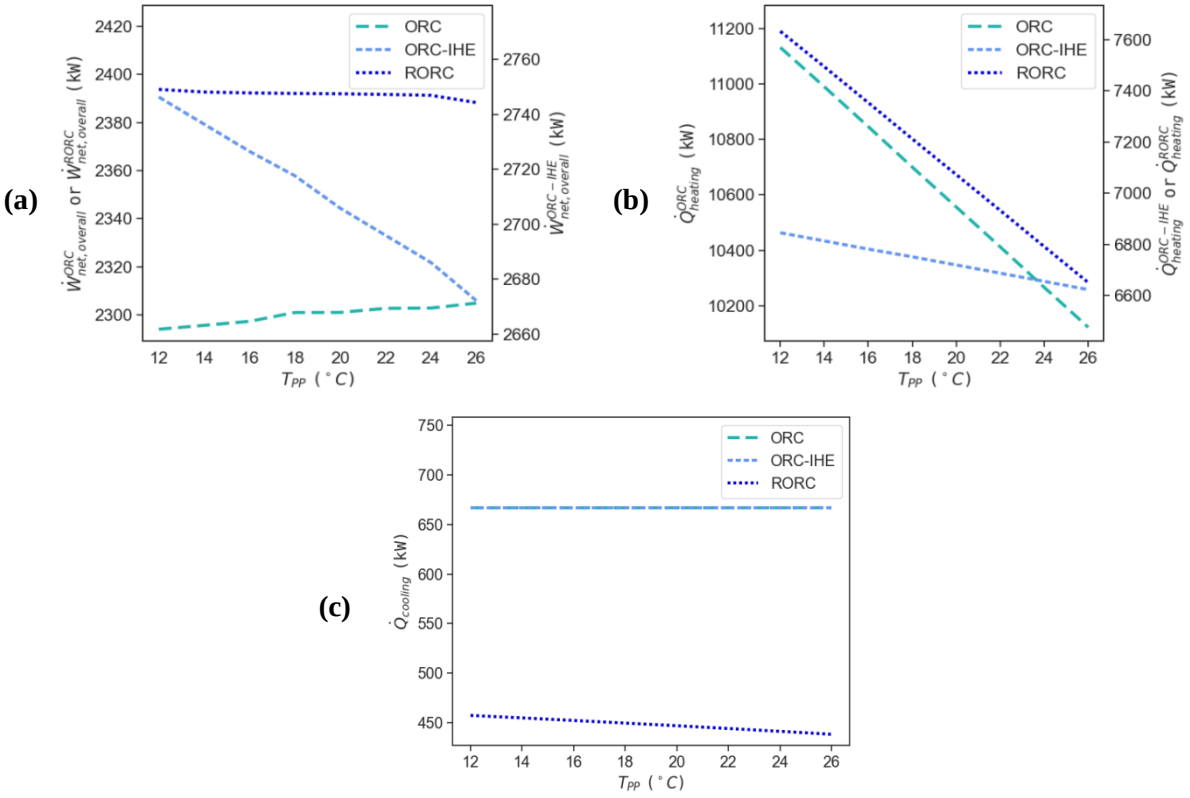

Figure 2. Effect of ORC evaporator pinch point temperature on the power outputs of the hybrid systems, in terms of: a) overall net electrical power; b) heating power; c) cooling power.

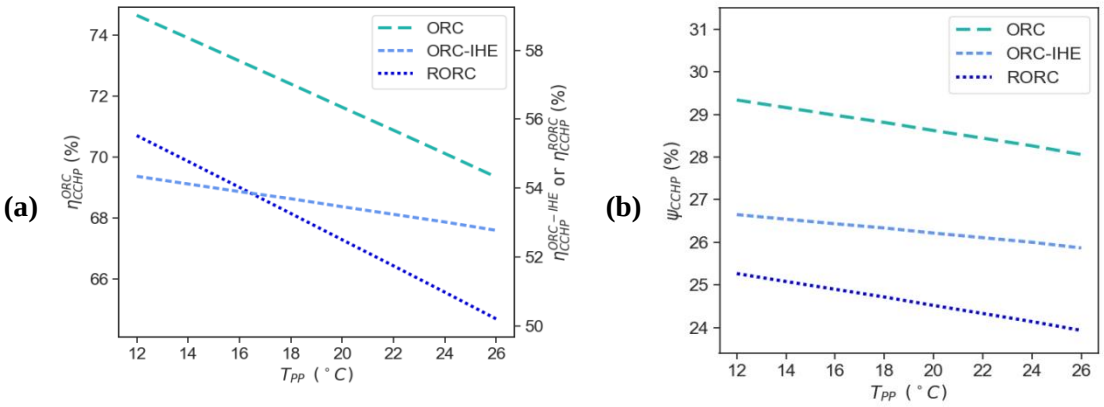

Figure 3. Effect of ORC evaporator pinch point temperature on the overall energy and exergy efficiencies of three proposed configurations.

enhancement rate of $\dot{W}_{net}^{KCS}$ in the ORC based configuration slightly dominates the reduction rate of $\dot{W}_{net}^{ORC}$ which increases $\dot{W}_{net,overall}$ by 0.5 % for 14 ℃ rise of T_{PP}. In contrast, the ORC-IHE and RORC based systems experience an opposite trend leading to reduction of $\dot{W}_{net,overall}$ by 2.7 % and 0.2 %, respectively.

Figure 2 also shows that by increase of T_{PP}, the heating power declines in all three hybrid systems, such that 14 ℃ rise of T_{PP} in the ORC, ORC-IHE, and RORC based systems decreases the heating power by 9 %, 3.24 %, and 12.85 %, respectively. This drop is due to reduction of input energy to the ORC and therefore to the HP unit. The heating exergy also decreases for all systems.

Regarding the cooling power of the ORC and ORC-IHE based systems, neither the mass flow rate through the HPG nor the state conditions at its inlet and outlet depend on T_{PP}. Consequently, change of ORC evaporator pinch point temperature does not affect the cooling power of these two systems (as can be observed in Figure 2) and as a result, the cooling exergy remains constant as well. In contrast, increase of T_{PP} in the RORC based system grows the mass flow rate bleeding towards the FFH and reduces the mass flow rate passing through the HPG. This reduces the cooling power by 4.15 % for 14 ℃ increase of T_{PP}. The cooling exergy of the RORC system is decreased as well.

Figures 3 illustrates variation of overall energetic and exergetic efficiencies of the trigeneration systems with T_{PP}. The input energy and exergy to all systems are identical. Since the heating power and exergy of all trigeneration systems decrease for an increase of the ORC evaporator pinch point temperature, the CCHP efficiency (both in energy and exergy viewpoints) reduce for all three configurations. More specifically, for 14 ℃ growth of T_{PP}, the ORC, ORC-IHP and RORC based systems experience 7.1, 2.89 and 9.58 percent drop in the energetic CCHP efficiency and 4.36, 2.94 and 5.28 percent decline in the exergetic CCHP efficiency, respectively.

5.1.2 ORC pump inlet temperature

The ORC pump inlet temperature (T_{32}) also affects energetic and exergetic characteristics of the proposed systems. This effect is investigated for various values of T_{32} in the range of $115 - 145$ ℃, based on the fixed ORC evaporator pinch point temperature and turbine inlet pressure (20 ℃ and 2 MPa, respectively).

Figure 4 illustrates the impact of variation of T_{32} on the power outputs of the trigeneration systems in terms of electrical, heating and cooling effects. In the case of ORC and ORC-IHE based

systems, increase of T_{32} reduces the heat absorption by the ORC evaporator leading to enhanced input energy to the KCS evaporator. A higher temperature at the ORC evaporator inlet is responsible for such trend. Because of constant pressure of FFH in the RORC based system, the OWF temperature at the RORC evaporator inlet is independent to the pump inlet temperature. Therefore, the heat transferred to the RORC cycle (and in turn the heat flow towards the KCS) is unchanged by variation of T_{32}. Consequently, by increase of the ORC pump inlet temperature, the difference between the highest and lowest temperatures of all ORC based systems decreases, which leads to reduction of $\dot{W}_{net}^{ORC}$. In addition, increase of T_{32} in the ORC and ORC-IHE based systems decreases the input thermal energy and exergy to the ORC cycle while increases the energy and exergy transfer to the KCS cycle and consequently enhances $\dot{W}_{net}^{KCS}$ as well. Based on the calculations, reduction rate of $\dot{W}_{net}^{ORC}$ dominates the growth rate of $\dot{W}_{net}^{KCS}$, causing 13.7 % drop in the net electrical power generated by both ORC and ORC-IHE based systems. In contrast, increase of T_{32} in the RORC system makes no change in $\dot{Q}_{ev}^{ORC}$ and $\dot{Q}_{ev}^{KCS}$, that in turn leads to the same KCS power for various ORC pump inlet temperatures. Because of reduction of $\dot{W}_{net}^{ORC}$ in the RORC system, an increase in T_{32} decreases $\dot{W}_{net,overall}$ by 10.57 %.

The enthalpy difference between inlet and outlet of the HP unit and HPG (the ORC side) decreases by increase of T_{32} for all trigeneration configurations. In the ORC and ORC-IHE systems, this causes decline of the heating and cooling power rates in both energy and exergy viewpoints, as shown in Figure 4. In the case of RORC system, the mass flow rate through the HP unit and HPG

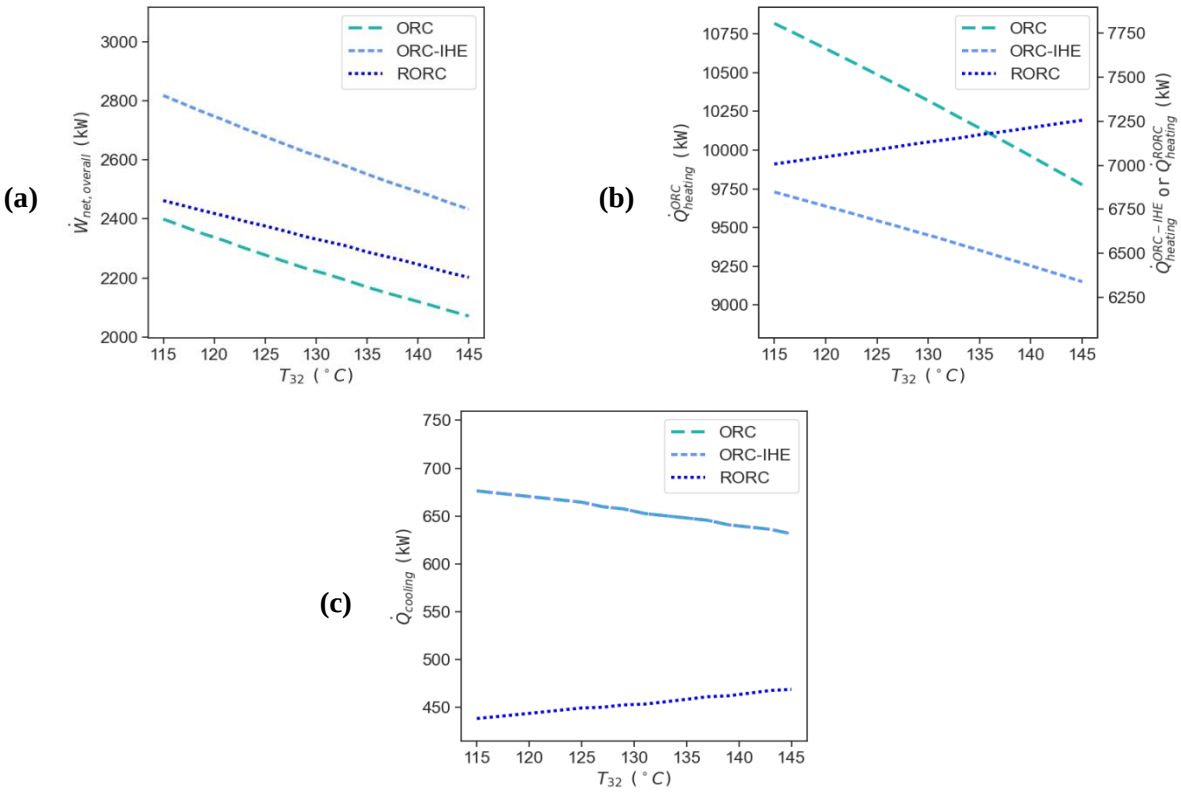

Figure 4. Effect of the ORC pump inlet temperature on the system outputs for three trigeneration systems, in terms of: a) overall net electrical power; b) heating power; c) cooling power.

grows by increase of T_{32}. This dominates the descending trend mentioned for the enthalpy difference of these components, causing 3.54 % and 6.95 % enhancement in the heating and cooling powers, respectively. The same trend also happens for exergetic powers of the RORC system.

Figure 5 examines the effect of ORC pump inlet temperature on the overall energetic and exergetic efficiencies of the three trigeneration systems. Regarding the energetic CCHP efficiency, Figure 5 indicates 10.19 % and 9 % decline in the performance of ORC and ORC-IHE systems, respectively while there is 0.18 % efficiency enhancement for the RORC system. The latter improvement is due to domination of ascending trend of $\dot{Q}_{cooling}$ and $\dot{Q}_{heating}$ to the descending trend of $\dot{W}_{net,overall}$ by increase of T_{32}. However, in the case of exergetic CCHP efficiency for the RORC system, the ascending rate of $\dot{E}x_{cooling}$ and $\dot{E}x_{heating}$ could not surpass the descending rate of $\dot{W}_{net,overall}$, and consequently Ψ_{CCHP} in RORC system decreases in the same manner as the other two trigeneration systems. More specifically, there are 12.05 %, 11.93 % and 5.53 % drop of exergetic CCHP efficiency for the ORC, ORC-IHE and RORC based systems by 30 ℃ increase of the ORC pump inlet temperature.

5.2. Performance comparison with the literature

This section compares thermodynamic performance of the proposed systems with related results of the literature. T_{PP}, T_{32} and $\dot{m}_{OWF}$ are considered to be 20 ℃, 123 ℃ and 20 kg/s, respectively. Two PTSC-driven hybrid systems are considered as follows.

1. Eisavi et al. [15] analyzed a PTSC-driven CCHP system integrated with direct-fed ORC, a DEARC system as the bottoming cycle, and two HP unit (one was fed by ORC (HP1) and the other was supplied by solar HTF (HP2)). Electrical, CHP and CCP exergy efficiencies of this hybrid system were 4.4 %, 12.8 % and 4.5 %, respectively, which are lower than respective efficiencies of the proposed ORC based system in the present study, i.e. 15.19 %, 28.34 % and 15.47 %. Substitution of HP2 with KCS system is the main reason for enhanced performance of the current study. Incorporating the KCS system into the CCHP system improves its electrical power and efficiency. Moreover, KCS evaporator results in less exergy destruction compared to HP2, owing to a better thermal match of ammonia-water mixture in the KCS evaporator with the heat source (solar HTF) compared to pure water in HP2 [45].

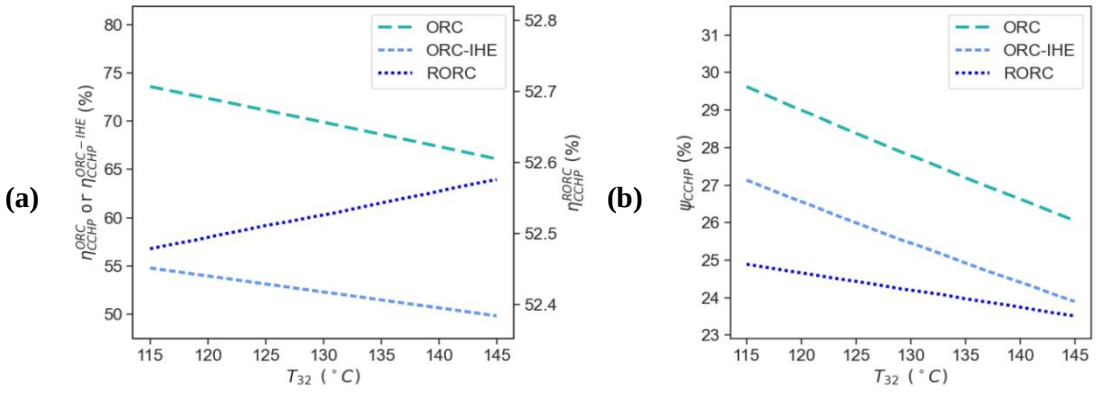

Figure 5. Effect of ORC pump inlet temperature on the overall energy and exergy efficiencies of three proposed configurations.

2. Tariq et al. [24] evaluated a hybrid system consisting of PTSC-driven ORC and DEARC cycles integrated with KCS as the bottoming system. The highest energetic efficiency was reported as 46.30 %, which is lower than those achieved in the current study for ORC, ORC-IHE and RORC based systems, i.e. 71.64 %, 53.46 % and 52.5 %, respectively. This is due to modification of DEARC configuration to a bottom-cycle arrangement feeding by ORC (the present study) instead of direct feeding by solar HTF (the study of Tariq et al.). Although such configuration may decline the cooling capacity, it supplies more input energy for both ORC and KCS systems and improves net electrical power and overall efficiency of the tri-generation system. The literature also confirms improvement of the efficiency of multi-generation systems when ARC system is configured as a bottoming cycle instead of a direct-fed arrangement [11, 25, 26].

Overall, the above comparison indicates higher thermodynamic performance of the proposed hybrid systems in comparison with the previous related research.

6. Conclusion

The current study investigated the impact of key parameters of ORC cycle on the performance of a novel energy distribution based on direct-fed ORC and bottom-cycled arrangement of DEARC and KCS for the PTSC-driven tri-generation system. Based on such configuration, three new tri-generation systems involving three different ORC structures (simple, regenerative, and ORC integrated with IHE) were proposed. Effect of key ORC parameters namely ORC evaporator pinch point temperature and pump inlet temperature on the thermodynamic performance of trigeneration systems was examined.

Increase of ORC evaporator pinch point temperature in all three systems reduced the heat input towards the ORC evaporator while grew that of the KCS evaporator. For ORC-IHE and RORC based systems, increase of T_{PP} decreased the overall net electrical power, while this characteristic was enhanced in the ORC based system. Additionally, increase of T_{PP} reduced the heating power, and energetic/exergetic CCHP efficiencies for all trigeneration systems. This also decreased the cooling power of the RORC based system, though it did not affect the cooling power in the ORC and ORC-IHE based systems.

In the ORC and ORC-IHE based systems, increase of ORC pump inlet temperature decreased the heat input towards the ORC evaporator while increased that of the KCS evaporator, whereas the RORC based system did not alter the energy distribution between ORC and KCS sub-systems. Regarding the impact of the increase of ORC pump inlet temperature on the systems characteristics, except for the heating/cooling power and energetic CCHP efficiency in the RORC based system, the trends were descending for all characteristics of the three proposed trigeneration systems.

Nomenclature

A	Area (m^2)	el	Electrical
C	Concentration ratio	ev	Evaporator
c_P	Specific heat capacity ($kJ/kg\,.K$)	fm	Film
D	Diameter (m)	g	Generator
Ex	Exergy (kJ)	HP	Heating process
$\dot{Ex}$	Exergy rate (kW)	in	Inlet
F	Focal length (m)	m	Motor
G	Solar irradiation (kW/m^2)	max	Maximum
H	Specific enthalpy (kJ/kg)	opt	Optimum
K	Thermal conductivity ($W/m^2\,.K$)	r	Receiver
L	Collector length (m)	ri	Receiver inner surface
N	Number of collector rows	ro	Receiver outer surface
$\dot{m}$	Mass flow rate (kg/s)	s	Solar
P	Pressure	t	Total
$\dot{Q}$	Heat rate (kW)	tur	Turbine
T	Temperature	u	Useful
V	Velocity (m/s)	***Abbreviations***	
W	Collector width (m)	ARC	Absorption refrigeration cycle
$\dot{W}$	Power rate (kW)	CCHP	Combined cooling, heat and power
X	Concentration	CCP	Combined cooling and power
Greek symbols		CHP	Combined heat and power
α	Absorptivity	COP	Coefficient of performance
γ	Intercept factor	DEARC	Double-effect absorption refrigeration cycle
ε	Emissivity	EV	Expansion valve
η	Energy efficiency (%)	FFH	Feed fluid heater
θ	Incident angle	HP	Heating process
μ	Dynamic viscosity	HPG	High pressure generator
ρ	Reflectivity	HTF	Heat transfer fluid
σ	Stefan-Boltzmann constant ($W/m^2\,.K^4$)	HTHE	High temperature heat exchanger
τ	Transmissivity	IHE	Internal heat exchanger
ψ	Exergy efficiency (%)	KCS	Kalina cycle system
Subscripts		LPG	Low pressure generator
am	Ambient	LTHE	Low temperature heat exchanger
b			
ap	Aperture	ORC	Organic Rankine cycle
b	Beam	OWF	Organic working fluid
c	cover	Pr	Prandtl number
ci	Cover inner surface	PTSC	Parabolic trough solar collector
co	Cover outer surface	Re	Reynolds number
coll	Collector	RORC	Regenerative organic Rankine cycle
con	Concentrator	SF	Solar field

References

[1] Bai, W.,X. Xu, Comparative analyses of two improved CO2 combinated cooling, heating, and power systems driven by solar energy, *Thermal Science*, *22*. (2018), Suppl. 2, pp. 693-700

[2] Kialashaki, Y., A linear programming optimization model for optimal operation strategy design and sizing of the CCHP systems, *Energy Efficiency*, *11*. (2018), pp. 225-238

[3] Haghghi, M.A., *et al.*, Thermodynamic assessment of a novel multi-generation solid oxide fuel cell-based system for production of electrical power, cooling, fresh water, and hydrogen, *Energy Conversion and Management*, *197*. (2019), p. 111895

[4] Li, P., *et al.*, A cascade organic Rankine cycle power generation system using hybrid solar energy and liquefied natural gas, *Solar Energy*, *127*. (2016), pp. 136-146

[5] Shuang, Y., *et al.*, ANALYSIS OF HEAT TRANSFER AND IRREVERSIBILITY OF ORGANIC RANKINE CYCLE EVAPORATOR FOR SELECTING WORKING FLUID AND OPERATING CONDITIONS, *Thermal Science*, *24*. (2020),

[6] Wang, Y., *et al.*, Thermodynamic performance comparison between ORC and Kalina cycles for multi-stream waste heat recovery, *Energy Conversion and Management*, *143*. (2017), pp. 482-492

[7] Shirazi, A., *et al.*, Solar-powered absorption chillers: A comprehensive and critical review, *Energy Conversion and Management*, *171*. (2018), pp. 59-81, DOI No. https://doi.org/10.1016/j.enconman.2018.05.091

[8] Bellos, E.,C. Tzivanidis, Parametric analysis and optimization of a solar driven trigeneration system based on ORC and absorption heat pump, *Journal of Cleaner Production*, *161*. (2017), pp. 493-509

[9] Ibrahim, A.,M. Kayfeci, Comparative analysis of a solar trigeneration system based on parabolic trough collectors using graphene and ferrofluid nanoparticles, *Thermal Science*, *25*. (2021), 4 Part A, pp. 2549-2563

[10] Gao, G., *et al.*, The study of a seasonal solar CCHP system based on evacuated flat-plate collectors and organic Rankine cycle, *Thermal Science*, *24*. (2020), 2 Part A, pp. 915-924

[11] Zhao, L., *et al.*, Solar driven ORC-based CCHP: Comparative performance analysis between sequential and parallel system configurations, *Applied Thermal Engineering*, *131*. (2018), pp. 696-706

[12] Bellos, E.,C. Tzivanidis, Dynamic investigation and optimization of a solar-fed trigeneration system, *Applied Thermal Engineering*, *191*. (2021), p. 116869

[13] Jafary, S., *et al.*, A complete energetic and exergetic analysis of a solar powered trigeneration system with two novel organic Rankine cycle (ORC) configurations, *Journal of Cleaner Production*, *281*. (2021), p. 124552

[14] Barbazza, L., *et al.*, Optimal design of compact organic Rankine cycle units for domestic solar applications, *Thermal Science*, *18*. (2014), 3, pp. 811-822

[15] Eisavi, B., *et al.*, Thermodynamic analysis of a novel combined cooling, heating and power system driven by solar energy, *Applied Thermal Engineering*, *129*. (2018), pp. 1219-1229

[16] Chen, Y., *et al.*, Exergo-economic assessment and sensitivity analysis of a solar-driven combined cooling, heating and power system with organic Rankine cycle and absorption heat pump, *Energy*, *230*. (2021), p. 120717

[17] Chen, Y., *et al.*, Performance analysis and exergo-economic optimization of a solar-driven adjustable tri-generation system, *Energy Conversion and Management*, *233*. (2021), p. 113873

[18] Cao, Y., *et al.*, Performance enhancement and multi-objective optimization of a solar-driven setup with storage process using an innovative modification, *Journal of Energy Storage*, *32*. (2020), p. 101956

[19] Han, Z., *et al.*, Thermodynamic performance analysis and optimization for a novel full-spectrum solar-driven trigeneration system integrated with organic Rankine cycle, *Energy Conversion and Management*, *245*. (2021), p. 114626

[20] Xi, Z., *et al.*, Energy, exergy, and exergoeconomic analysis of a polygeneration system driven by solar energy with a thermal energy storage tank for power, heating, and freshwater production, *Journal of Energy Storage*, *36*. (2021), p. 102429

[21] Ganesh, S.N.,T. Srinivas, Processes development for high temperature solar thermal Kalina power station, *Thermal Science*, *18*. (2014), suppl. 2, pp. 393-404

[22] Gogoi, T.,P. Hazarika, Comparative assessment of four novel solar based triple effect absorption refrigeration systems integrated with organic Rankine and Kalina cycles, *Energy Conversion and Management*, *226*. (2020), p. 113561
[23] Almatrafi, E., *et al.*, Thermodynamic investigation of a novel cooling-power cogeneration system driven by solar energy, *International Journal of Refrigeration*, *138*. (2022), pp. 244-258
[24] Tariq, S., *et al.*, Exergy-based weighted optimization and smart decision-making for renewable energy systems considering economics, reliability, risk, and environmental assessments, *Renewable and Sustainable Energy Reviews*, *162*. (2022), p. 112445
[25] Chen, K., *et al.*, Thermodynamic and economic comparison of novel parallel and serial combined cooling and power systems based on sCO2 cycle, *Energy*, *215*. (2021), p. 119008
[26] Tzivanidis, C.,E. Bellos, A comparative study of solar-driven trigeneration systems for the building sector, *Energies*, *13*. (2020), 8, p. 2074
[27] Kerme, E.D., *et al.*, Energetic and exergetic performance analysis of a solar driven power, desalination and cooling poly-generation system, *Energy*, *196*. (2020), p. 117150
[28] Florides, G.A., *et al.*, Modelling and simulation of an absorption solar cooling system for Cyprus, *Solar energy*, *72*. (2002), 1, pp. 43-51
[29] Kalogirou, S., Recent patents in absorption cooling systems, *Recent Patents on Mechanical Engineering*, *1*. (2008), 1, pp. 58-64
[30] Sheikhani, H., *et al.*, A review of solar absorption cooling systems combined with various auxiliary energy devices, *Journal of Thermal Analysis and Calorimetry*, *134*. (2018), 3, pp. 2197-2212
[31] Price, H., *et al.*, Advances in parabolic trough solar power technology, *J. Sol. Energy Eng.*, *124*. (2002), 2, pp. 109-125
[32] Yaws, C.L., *et al.*, Heat Capacity of Gas, *Chemical Properties Handbook*. (1999),
[33] Avanessian, T.,M. Ameri, Energy, exergy, and economic analysis of single and double effect LiBr–H2O absorption chillers, *Energy and Buildings*, *73*. (2014), pp. 26-36
[34] Al-Oran, O., *et al.*, Exergy and energy amelioration for parabolic trough collector using mono and hybrid nanofluids, *Journal of Thermal Analysis and Calorimetry*. (2020), pp. 1-18
[35] Bellos, E.,C. Tzivanidis, Analytical expression of parabolic trough solar collector performance, *Designs*, *2*. (2018), 1, p. 9
[36] Ghaebi, H., *et al.*, Energy, exergy and exergoeconomic analysis of a cogeneration system for power and hydrogen production purpose based on TRR method and using low grade geothermal source, *Geothermics*, *71*. (2018), pp. 132-145
[37] Haghghi, M.A., *et al.*, Thermodynamic investigation of a new combined cooling, heating, and power (CCHP) system driven by parabolic trough solar collectors (PTSCs): A case study, *Applied Thermal Engineering*, *163*. (2019), p. 114329
[38] Al-Sulaiman, F.A., *et al.*, Exergy modeling of a new solar driven trigeneration system, *Solar Energy*, *85*. (2011), 9, pp. 2228-2243
[39] Malaine, S., *et al.*, Advanced exergetic study to assess the effects of rectification and distillation on absorption refrigerators, *Thermal Science*. (2022), 00, pp. 147-147
[40] Wang, S., *et al.*, Assessment of an integrated solar combined cycle system based on conventional and advanced exergetic methods, *Thermal Science*, *26*. (2022), 5 Part A, pp. 3923-3937
[41] Bellos, E., *et al.*, Parametric investigation and optimization of an innovative trigeneration system, *Energy Conversion and Management*, *127*. (2016), pp. 515-525
[42] Dudley, V.E., *et al.*, Test results: SEGS LS-2 solar collector, 'Report, Sandia National Lab.(SNL-NM), Albuquerque, NM (United States), 1994.
[43] Safarian, S.,F. Aramoun, Energy and exergy assessments of modified Organic Rankine Cycles (ORCs), *Energy reports*, *1*. (2015), pp. 1-7
[44] He, J., *et al.*, Performance research on modified KCS (Kalina cycle system) 11 without throttle valve, *Energy*, *64*. (2014), pp. 389-397
[45] Blanco, M.,L.R. Santigosa, *Advances in concentrating solar thermal research and technology*. Woodhead Publishing, 2016.

Submitted: 17.06.2023
Revised: 07.08.2023
Accepted: 16.08.2023